

# Unveiling causal activity of complex networks

Rashid V. Williams-García,\* John M. Beggs, and Gerardo Ortiz  
*Department of Physics, Indiana University, Bloomington, Indiana 47405, USA*  
(Dated: March 17, 2016)

We introduce a novel tool for analyzing complex network dynamics, allowing for cascades of causally-related events, which we call causal webs (c-webs), to be separated from other non-causally-related events. This tool shows that traditionally-conceived avalanches may contain mixtures of spatially-distinct but temporally-overlapping cascades of events, and dynamical disorder or noise. In contrast, c-webs separate these components, unveiling previously hidden features of the network and dynamics. We apply our method to mouse cortical data with resulting statistics which demonstrate for the first time that neuronal avalanches are not merely composed of causally-related events.

PACS numbers: 87.19.lc, 64.60.av, 87.19.lj, 64.60.aq

In systems consisting of many interacting elements, a variety of methods (e.g., transfer entropy or Granger causality) are often used to reveal hidden dynamical causal links between them. This naturally leads to a complex networks description [1], raising interesting questions. For example, what fraction of the activity in such a network can be attributed to the hidden causal dynamics, and what fraction is produced by other processes, such as noise? Here we describe a new approach to this problem and demonstrate its utility on neural networks.

Over the past twenty years, there have been a number of theoretical [2–14] and experimental [15–27] attempts to connect activity in living neural networks to critical avalanches like those seen in the Bak-Tang-Wiesenfeld (BTW) sandpile model [28, 29]. It has been hypothesized that homeostatic mechanisms might *tune* the brain, a complex neural network, towards optimality associated with a critical point [30] which separates ordered (“supercritical”) and disordered (“subcritical”) phases, where cascades of activity are amplified or damped, respectively [14, 23, 26, 31, 32]. In the BTW model, grains of “sand” are dropped one at a time at random lattice locations; sites which reach a threshold height topple their grains to their neighboring sites, potentially inducing further topplings, together forming an emergent cascade of events called an avalanche. Successive topplings are thus causally related, with each new toppling having been induced by another which happened before. The sandpile model eventually reaches a steady state in which the probability distribution of avalanche sizes is a power law, a potential indicator of criticality. It is important to note that the grains are dropped at an infinitesimally slow rate such that the relaxation timescale, i.e., the duration of the avalanches, is much shorter than the time between grain drops. This *separation of timescales* is essential to this concept of self-organized criticality (SOC) [2].

In real systems, however, this separation is not always achieved. As we will see, closer inspection of experimental neuronal avalanche data reveals potential conflicts with the SOC approach. For example, temporally distinct avalanches could be concatenated by spontaneous

activity occurring between them, or two spatially distinct avalanches could be concatenated if they occurred at overlapping times. These confounding situations highlight the need for a method to clearly separate causally from non-causally related activity.

Recent work developed a framework in which there is no separation of timescales [33]. It has been demonstrated that access to criticality relates to the coupling of the concerned network to an external environment, resulting in a non-zero spontaneous activation probability; the higher the probability, the further from criticality, and thus the further from optimality [33]. Spontaneous activity is not necessarily intrinsic to the network, but perhaps originates due to a coupling with an environment. Indeed, spontaneous events such as these could be caused by some unobserved influence, *noise*, (in which case the network has been undersampled) or by intrinsic properties of the neurons themselves, such as those neurons which have a propensity to fire spontaneously or are tonically active, e.g., as in the case of pacemaker cells or some inhibitory neurons [34, 35]. Vanishing spontaneous activity is equivalent to a separation of timescales, as described in SOC. Thus, achieving optimality by operating at a critical point may not be feasible for a living, open neural network, according to the quasicriticality hypothesis introduced in [33], although a relative optimality may still be achieved along a nonequilibrium Widom line. The accessibility of this relatively-optimal quasicritical region will likely depend on the character of the environment and the fundamental properties of the neural network itself. Our ability to apply the nonequilibrium Widom line framework and test the quasicriticality hypothesis, however, hinges on the ability to identify spontaneous activity in a living neural network. In this paper, we introduce a method to disentangle spontaneous neuronal activity from that which is causally-related and primarily governed by the network structure and dynamics. We focus our attention on directed networks, such as those found in living neural networks.

We next introduce the notion of **causal webs** (or c-webs for short), as a new emergent cascade of correlated

events, whose properties contrast and complement those of standard avalanches. Whereas the latter are defined as spatiotemporal patterns of activation spanning a number of adjacent time steps framed by time steps lacking activity, c-webs explicitly depend on the network structure and temporal delays, thus accommodating the potential non-Markovian dynamics of complex networks. Knowledge of the network structure and delay information is key, as it allows to distinguish between different spatiotemporal patterns of activation in a way which is not possible with avalanches (see Fig. 1).

Let us formalize the concept of c-webs in the context of neural networks. We label individual events by  $x = (i, t)$ , representing the activation of neuron  $i$  at time  $t$ , or following the notation used in [33],  $z_i(t) = 1$  ( $z_i(t) = 0$  meant quiescence). We write the set of all events  $A = \{x_\mu\}$ , e.g., in Fig. 1B,  $A = \{a, b, c, d, e, f, g\}$ . Formally, we define a c-web  $C$  as a set of correlated ordered pairs  $(x_\nu^{(1)}, x_\nu^{(2)})$  of events (i.e., spikes), which we call **causal pairs**; quiescent neurons are not included in the set. The first and second entries,  $x_\nu^{(1)}$  and  $x_\nu^{(2)}$ , of the  $\nu$ th causal pair represent causally-related presynaptic and postsynaptic events, respectively. (Despite causal relations being made in a pairwise fashion, we emphasize that this does not preclude multivariate interactions, as multiple pairings can be made to a single event.) In the following, we show how to determine those causal pairs.

A complete set of causal pairs  $X$  is constructed by taking the Cartesian product of each event  $x_\mu$  with its corresponding **dynamic postsynaptic events**  $\mathcal{U}(x_\mu)$ ,

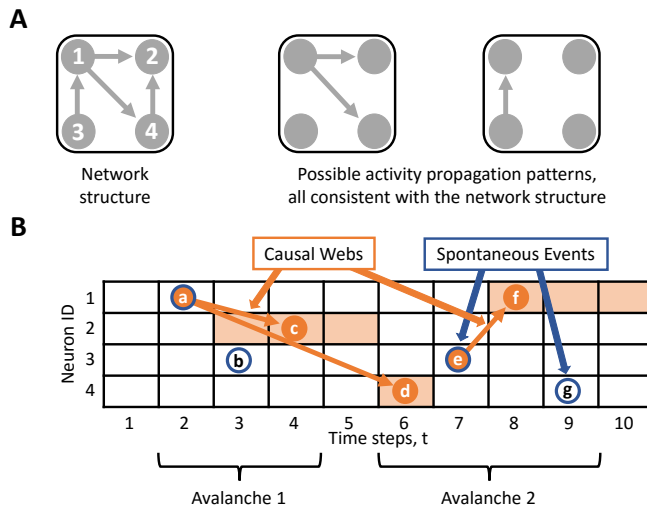


FIG. 1. (Color online) Causal webs are distinct from neuronal avalanches in that they rely on network structure and synaptic delays. **A.** A network produces a variety of spatiotemporal activity patterns. **B.** Whereas only two neuronal avalanches are detected, a richer structure is revealed when spontaneous events (blue annuli) are separated from c-webs (orange disks); acceptance windows  $W_{ij}(t)$  are shaded light-orange.

i.e.,  $X = \bigcup_{x_\mu \in A} x_\mu \times \mathcal{U}(x_\mu)$ , where  $\mathcal{U}(x) \equiv \mathcal{U}(i, t)$  is the set given by

$$\mathcal{U}(i, t) = \{(j, t') \mid j \in N(i) \text{ and } t' \in W_{ij}(t)\}. \quad (1)$$

$N(i)$  refers to the set of all postsynaptic neurons  $j$  of neuron  $i$ , and  $W_{ij}(t) = [t + d_{ij} - \Delta_{ij}, t + d_{ij} + \Delta_{ij}]$  is a predetermined dynamical **acceptance window**: if a postsynaptic neuron  $j$  is active within the acceptance window, then a causal link is inferred. The lower bound of the acceptance window is adjusted such that it is greater than  $t$ . We write the set of events in  $X$  as  $A(X) \subseteq A$ .

Synaptic delays  $d_{ij}$  associated with the connection from a presynaptic neuron  $i$  to a postsynaptic neuron  $j$ , are allowed to have some uncertainty  $\Delta_{ij}$  due to variability in the postsynaptic spike timing. We will later present a method by which this information can be determined from data; for the moment, we assume it is given. In Fig. 1B, synaptic delays and their uncertainties are given for the connections in Fig. 1A:  $d_{12} = 2$ ,  $d_{14} = 4$ ,  $d_{31} = 2$ , and  $d_{42} = 1$ , with  $\Delta_{12} = 1$ ,  $\Delta_{14} = 0$ ,  $\Delta_{31} = 1$ , and  $\Delta_{42} = 1$ . This information can be used to determine causal pairs, e.g., the event  $a = (1, 2)$  in Fig. 1B has  $\mathcal{U}(a) = \{c, d\}$ , resulting in the causal pairs  $a \times \mathcal{U}(a) = \{(a, c), (a, d)\}$ . The complete set of causal pairs for the **spacetime graph** in Fig. 1B is  $X = \{(a, c), (a, d), (e, f)\}$  and so  $A(X) = \{a, c, d, e, f\}$ .

A causal web represents the connected components of a directed graph whose vertices and edges are  $A(X)$  and  $X$ , respectively. The example in Fig. 1B thus has two c-webs,  $C_1 = \{(a, c), (a, d)\}$  and  $C_2 = \{(e, f)\}$ . Note that spontaneous events initiate c-webs and may become part of ongoing c-webs. The **size**  $s(C)$  of a c-web is defined as the total number of distinct events within it. Defining that set as  $A(C)$ , the size  $s(C)$  is then given by its cardinality:  $s(C) = |A(C)|$ . Note that  $A(C) \subseteq A(X)$ . For example,  $A(C_1) = \{a, c, d\}$  and  $A(C_2) = \{e, f\}$  in Fig. 1B, with  $s(C_1) = 3$  and  $s(C_2) = 2$ , respectively.

The **duration**  $D(C)$  of a c-web  $C$  can be defined in terms of its **chord**. The chord of a c-web  $K(C)$  is the sequence of distinct time steps for which there are events belonging to that c-web, arranged in ascending order in time, with no repeated elements. That is,  $K(C) = (t_1, t_2, \dots, t_n)$ , where  $t_1$  and  $t_n$  are the times of the first and last events, respectively. In contrast to the definition of duration for avalanches, the length of a c-web's chord is not equal to the c-web duration. Instead, we define the duration of a c-web as a measure of its chord plus one, i.e.,  $D(C) = 1 + \lambda(K(C))$ , where  $\lambda(K(C)) = t_n - t_1$ . The chords of the c-webs in Fig. 1B, for example, are  $K(C_1) = (2, 4, 6)$  and  $K(C_2) = (7, 8)$ , with durations  $D(C_1) = 5$  and  $D(C_2) = 2$ .

Finally, we define the **branching fraction**  $\phi(C)$  of a c-web  $C$  as the average number of postsynaptic events

associated with each presynaptic event:

$$\phi(C) = \frac{1}{s(C)} \sum_{\mu=1}^{|A(C)|} \sum_{\nu=1}^{|C|} \delta_{x_{\mu}(C), x_{\nu}^{(1)}(C)}, \quad (2)$$

where  $\delta$  is the Kronecker delta. The first sum is evaluated over all events  $x_{\mu}(C)$  of c-web  $C$ , while the second one is over all presynaptic events  $x_{\nu}^{(1)}(C)$ , given by  $\beta(C) = \{x_{\nu}^{(1)}(C)\}$ . For example, in Fig. 1B,  $\beta(C_1) = \{a\}$  and  $\beta(C_2) = \{e\}$ , with  $\phi(C_1) = 2/3$  and  $\phi(C_2) = 1/2$ .

We performed tests of our method using simulations of the cortical branching model (CBM) [33]. Neuronal avalanches and c-webs should coincide as emergent cascades of correlated events in the limits  $p_s \rightarrow 0$  and  $d_{ij} = 1$  for all pairs of nodes  $(i, j)$ . We simulated  $10^6$  avalanches on a network of  $N = 243$  nodes, whose structure and synaptic weights were inspired by experimental data; all synaptic delays were set to a single time step. To simulate the  $p_s \rightarrow 0$  limit (a separation of timescales), we initiated avalanches at single, random nodes, only starting a new avalanche when the previous one had finished; no spontaneous events or concurrent avalanches were allowed. The resulting avalanche and c-web size probability distributions were identical, as expected.

In another test, we constructed a random network of  $N = 360$  nodes, each with an in-degree of  $k_{in} = 3$ , as in [33]. The network was reducible and had a Perron-Frobenius eigenvalue of  $\kappa = 0.23$  [33]. Synaptic delays (in time steps) were drawn from a uniform distribution of integers in a closed interval,  $d_{ij} \in [1, 16]$ . Spontaneous activation probabilities for each node were drawn from a

Gaussian distribution with mean and standard deviation of  $10^{-4}$ ; negative values were set to zero. The simulation was performed over  $3.6 \times 10^6$  time steps. Spontaneous events detected by our method were used to construct a new spontaneous activation probability distribution, which we compared with the initial distribution using a Kolmogorov-Smirnov test: the distributions were in agreement at a 5% significance level with a p-value of 0.9955 [37]. We note that as the overall connectivity of the network (which we quantify by  $\kappa$ , as in [33]) is increased, spontaneous events become less prominent as c-webs begin to dominate the dynamics, leading to more driven activations and refractory nodes, thus preventing spontaneous events: neural network dynamics present a fluctuating bottleneck to the influence of an environment.

To determine the c-webs, we have so far assumed knowledge of the network structure and delay information (i.e., the  $d_{ij}$  and  $\Delta_{ij}$ 's), however in practice, this information must be learned from experimental data. We now describe a method, based on delayed transfer entropy (TE) [38, 39], by which this information can be established from high temporal resolution multiunit time-series data. The use of TE is not absolutely necessary; alternatives (e.g., computing conditional probabilities directly from data) may be used so long as they provide a network structure and synaptic delays.

For a particular pair of neurons  $(i, j)$ , TE is calculated at various synaptic delays  $d$ , peaking at the appropriate  $d = d_{ij}$ , with a width of  $\Delta_{ij}$  [38]. At a given  $d$ , the TE from neuron  $i$  to neuron  $j$ , is given by

$$T_{i \rightarrow j}(d) = \sum_{\mathbf{z}_{i \rightarrow j}(d)} p(z_j(t-1), z_j(t), z_i(t-d)) \log_2 \left( \frac{p(z_j(t)|z_j(t-1), z_i(t-d))}{p(z_j(t)|z_j(t-1))} \right), \quad (3)$$

where  $\mathbf{z}_{i \rightarrow j}(d) = \{z_j(t-1), z_j(t), z_i(t-d)\}$  indicates that the sum is performed over all possible configurations of the binary variables  $z_j(t-1)$ ,  $z_j(t)$ , and  $z_i(t-d)$ . Joint and conditional probabilities in Eq. 3 are estimated from timeseries data [38]. Synaptic delay information from the delayed TE analysis is then used to infer the causal structure of the recorded activity, as in [40]. The method could be improved by converting TE values to activity transmission probabilities, as described in the supplemental materials of [41], and then stochastically accepting causal pairings of events depending on those probabilities.

We next demonstrate the utility of our method when applied to experimental data (see Fig. 2). For our demonstration, we have used ten data sets from [42], which were collected *in vitro* from organotypic cultures of mouse somatosensory cortex using a 512-microelectrode

array with a  $60 \mu\text{m}$  electrode spacing and a 20 kHz sampling rate over an hour-long recording [43, 44]. Data were spike-sorted to identify individual neurons and spurious connections have been removed, as in [40]. Using our method, spontaneous events (dark blue) were disentangled from c-webs (orange) to illustrate their qualitative differences. In Fig. 2A, we present an activity time raster (top panel) and corresponding timeseries of the activity (bottom panel), on which we have performed a moving average with a  $\Delta t = 100 \text{ ms}$  window:  $y(t) = \sum_{t'=0}^{\Delta t-1} x(t-t')/\Delta t$ , where  $x(t) = \sum_{i=1}^N \delta_{z_i(t), 1}$  [45]. In Fig. 2B, we plot logarithmically-binned avalanche and c-web size probability distributions for the data set best fit by a power law (log-likelihood  $L = -5.78 \times 10^5$  with  $s_{min} = 1$ ) to demonstrate that while neuronal avalanches may exhibit approximate power-law scaling, thus sug-

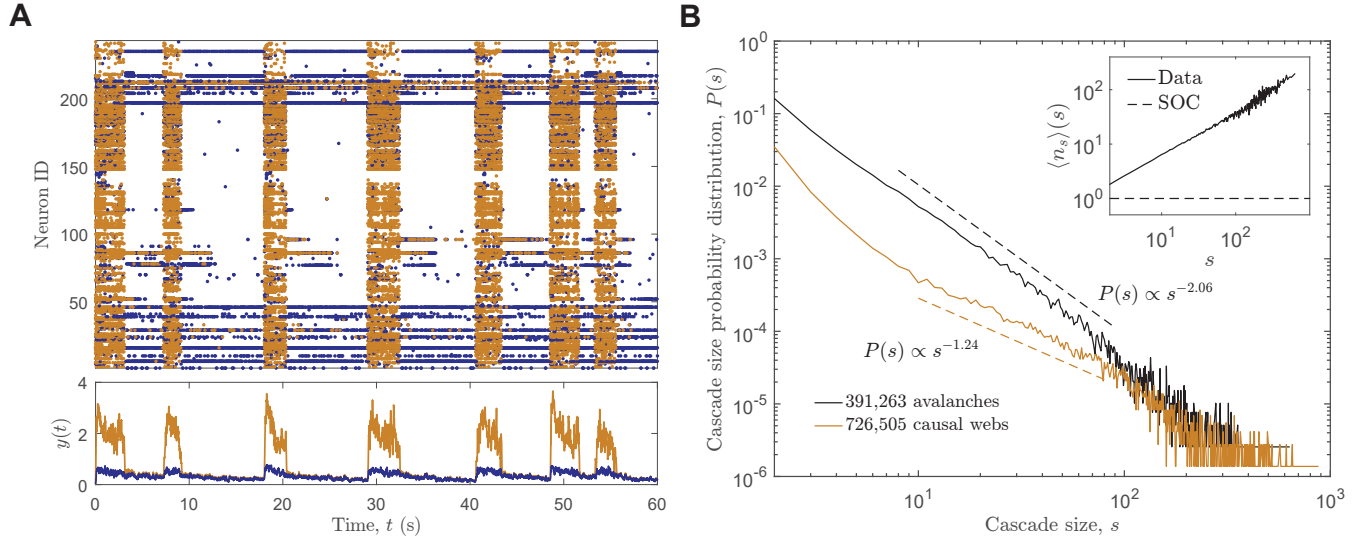


FIG. 2. (Color online) Application of the c-web method on experimental data. **A.** Time raster of one minute of neural network activity recorded from somatosensory cortex, processed to separate spontaneous events (dark blue) from c-webs (orange). Note that tonically-active neurons mainly produce spontaneous events. **B.** Avalanches binned at 1 ms (black) and c-webs (orange) exhibit different statistical properties and scaling; experimental data does not feature a separation of timescales (inset).

gesting underlying critical behavior, the corresponding c-web distribution does not ( $L = -8.12 \times 10^3$ ;  $s_{min} = 83$ ) [46]. Although we have not determined whether the data feature quasicritical dynamics, operating at or near the nonequilibrium Widom line, these results strongly suggest non-critical dynamics. To further illustrate how avalanches confound important dynamical information in the data, we plotted the average number of spontaneous events  $\langle n_s \rangle$  (identified using the c-webs method) as a function of the avalanche size  $s$  and compared this to results from simulations with a separation of timescales, where SOC would be applicable (see 2B inset).

Avalanche durations from experimental data followed approximate power laws with exponents in a range of [1.83, 3.38] and a median of 2.35; c-web duration distributions only marginally exhibited power-law behavior. Avalanche branching ratios were distributed around a mean of  $0.78 \pm 0.36$  and a median of 0.67; c-web branching fractions approximately ( $R^2 = 0.99$ ) followed an exponential distribution with an exponent  $-5.51 \pm 0.23$ .

The ability to disentangle c-webs from noise allows us to apply the nonequilibrium Widom line framework and discriminate criticality from quasicriticality [33], but also to examine the dynamics of living neural networks in novel ways. For example, it has been suggested that a reduced signal-to-noise ratio (SNR) produces inefficient hyperactivation in the prefrontal cortices of schizophrenics during successful cognitive tasks [47]. This hypothesis has been supported by computational models showing that neural network attractors become unstable with increased noise [48]. Thus c-webs could be used to examine the neural basis of hyperfrontality for the first

time. Another application is the identification of different classes of network nodes. For instance, because inhibitory neurons exhibit different firing patterns from excitatory neurons, namely fast-spiking and tonic activation [34, 35], and because we have found tonic activations to be mostly spontaneous (cf. Fig. 2A), distributions of spontaneous neuronal events may help identify inhibitory neurons, complementing previously-established methods [50]. This may provide further insight into the nature of rapid eye movement sleep, recently been shown to be induced by the activation of inhibitory neurons [49]. The latter may lead to a decreased SNR, as in the portions of Fig. 2A dominated by spontaneous events. Our method may also inform understanding of the neural network structure beyond the capabilities of currently available methods. In the case of network undersampling, hidden network cycles might be discovered by employing our approach in conjunction with population coupling methods [51]. Moreover, c-webs enable us to distinguish recurrent from feed-forward network dynamics. Finally, the use of c-webs obviates the need to choose a particular temporal binning, contrasting neuronal avalanches which depend strongly on the choice of binning [16, 17, 36]. These projects merit further investigation.

Similar applications could be envisioned for complex networks in general. For example, financial networks could be decomposed into agents that directly interact through exchanges as well as exogenous factors like weather or inflation. In models of disease spreading, such as the SIRS model, c-webs could differentiate between sources of infection [52]. Such an approach is likely to be useful whenever considering interacting units, whether

they are people in social networks, species in ecological webs, or protein molecules in a stochastic environment. A specific application in social media could involve the detection of Twitterbots and astroturfing [53].

The authors would like to thank Hadi Hafizi, Emily B. Miller, Benjamin Nicholson, and Zachary C. Tosi for valuable discussions, as well as Shinya Ito, Alan M. Litke, and Fang-Chin Yeh for providing their *in vitro* data.

---

\* Electronic address: rwgarcia@indiana.edu

[1] C. Gros, *Complex and Adaptive Dynamical Systems* (Springer-Verlag, Berlin, 2013).

[2] P. Bak, *How Nature Works: The Science of Self-Organized Criticality* (Springer-Verlag, New York, 1996).

[3] N. Bertschinger and T. Natschläger, *Neural Comput.* **16**, 1413 (2004).

[4] D. R. Chialvo, *Physica A* **340**, 756 (2004).

[5] C. Haldeman and J. M. Beggs, *Phys. Rev. Lett.* **94**, 058101 (2005).

[6] O. Kinouchi and M. Copelli, *Nat. Phys.* **2**, 348 (2006).

[7] A. Levina, J.M. Herrmann, and T. Geisel, *Nat. Phys.* **3**, 857 (2007).

[8] M. G. Kitzbichler et al., *PLoS Comput. Biol.* **5**, e1000314 (2009).

[9] W. Chen et al., *BMC Neurosci.* **11**, 3 (2010).

[10] D. B. Larremore et al., *Phys. Rev. Lett.* **106**, 058101 (2011).

[11] T. Mora and W. Bialek, *J. Stat. Phys.* **144**, 268 (2011).

[12] S. Pei et al., *Phys. Rev. E* **86**, 021909 (2012).

[13] K. Manchanda et al., *Phys. Rev. E* **87**, 012704 (2013).

[14] M. Rybarsh and S. Bornholdt, *PLoS ONE* **9**, e93090 (2014).

[15] G. A. Worrell et al., *Neuroreport* **13**, 2017 (2002).

[16] J. M. Beggs and D. Plenz, *J. Neurosci.* **23**, 11167 (2003).

[17] V. Pasquale et al., *Neuroscience* **153**, 1354 (2008).

[18] S. S. Poil, A. van Ooyen, and K. Linkenkaer-Hansen, *Hum. Brain Mapp.* **29**, 770 (2008).

[19] W. L. Shew et al., *J. Neurosci.* **29**, 15595 (2009).

[20] T. L. Ribeiro et al., *PLoS ONE* **5**, e0014129 (2010).

[21] W. L. Shew et al., *J. Neurosci.* **31**, 55 (2011).

[22] G. Solovey et al., *Front. Integr. Neurosci.* **6**, 44 (2012).

[23] V. Priesemann et al., *PLoS Comput. Biol.* **9**, e1002985 (2013).

[24] O. Shriki et al., *J. Neurosci.* **33**, 7079 (2013).

[25] S. Yu et al., *Front. Sys. Neurosci.* **7** (2013).

[26] L. de Arcangelis et al., *J. Stat. Mech.* **2014**, P03026

(2014).

[27] W. L. Shew et al., *Nat. Phys.* **11**, 659 (2015).

[28] P. Bak, C. Tang, and K. Wiesenfeld, *Phys. Rev. Lett.* **59**, 381 (1987).

[29] K. Christensen and N. R. Moloney, *Complexity and Criticality* (Imperial College Press, London, 2005).

[30] H. Nishimori and G. Ortiz, *Elements of Phase Transitions and Critical Phenomena* (Oxford, 2011).

[31] D. Hsu and J. M. Beggs, *Neurocomputing* **69**, 1134 (2006).

[32] B. A. Pearlmutter and C. J. Houghton, *Neural Comput.* **21**, 1622 (2009).

[33] R. V. Williams-García, M. Moore, J. M. Beggs, and G. Ortiz, *Phys. Rev. E* **90**, 062714 (2014).

[34] T. F. Freund and G. Buzsáki, *Hippocampus* **6**, 347 (1996).

[35] H. Hu et al., *Science* **345**, 1255263 (2014).

[36] D. Plenz et al., *Criticality in Neural Systems* (Wiley-VCH, Weinheim, 2014).

[37] F. James, *Statistical Methods in Experimental Physics* (World Scientific, Singapore, 2006).

[38] S. Ito et al., *PLoS ONE* **6**, e27431 (2011).

[39] M. Wibral et al., *PLoS ONE* **8**, e55809 (2013).

[40] S. Nigam et al., *J. Neurosci.* **36**, 670 (2016).

[41] N. Friedman, S. Ito, B. A. W. Brinkman, M. Shimono, R. E. L. DeVille, K. A. Dahmen, J. M. Beggs, and T. C. Butler, *Phys. Rev. Lett.* **108**, 208102 (2012).

[42] S. Ito, F. C. Yeh, N. M. Timme, P. Hottowy, A. M. Litke, and J. M. Beggs (2016), *Spontaneous spiking activity of hundreds of neurons in mouse somatosensory cortex slice cultures recorded using a dense 512 electrode array*. CR-CNS.org, <http://dx.doi.org/10.6080/K07D2S2F>

[43] A. M. Litke et al., *IEEE Transactions on Nuclear Science* **51**, 1434 (2004).

[44] S. Ito et al., *PloS ONE* **9**, e105324 (2014).

[45] A. V. Oppenheim et al., *Discrete-Time Signal Processing* (Prentice Hall, Englewood Cliffs, 1989).

[46] A. Clauset et al., *SIAM Review* **51**, 661 (2009).

[47] G. Winterer and D. R. Weinberger, *Trends Neurosci.* **27**, 683 (2004).

[48] E. T. Rolls et al., *Nature* **9**, 696 (2008).

[49] F. Weber et al., *Nature* **526**, 435 (2015).

[50] P. Barthó et al., *J. Neurophysiol.* **92**, 600 (2004).

[51] M. Okun et al., *Nature* **521**, 511 (2015).

[52] R.M. Anderson and R.M. May, *Nature* **280** (1979).

[53] J. Ratkiewicz, M. D. Conover, M. Meiss, B. Gonçalves, S. Patil, A. Flammini, and F. Menczer, “Truthy: mapping the spread of astroturf in microblog streams” in *Proceedings of the 20th international conference companion on world wide web* (ACM, New York, 2011), p. 249.